Journal Pre-proof

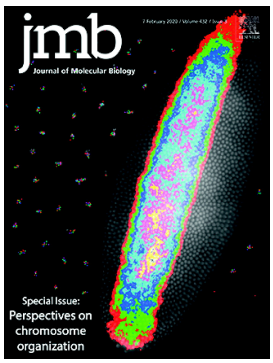

Systematic Transcriptional Profiling of Responses to STAT1- and STAT3-Activating Cytokines in Different Cancer Types

Mélanie Kirchmeyer, Florence Servais, Aurélien Ginolhac, Petr V. Nazarov, Christiane Margue, Demetra Philippidou, Nathalie Nicot, Iris Behrmann, Claude Haan, Stephanie Kreis

PII: S0022-2836(20)30553-2

DOI: https://doi.org/10.1016/j.jmb.2020.09.011

Reference: YJMBI 66652

To appear in: *Journal of Molecular Biology*

Received date: 20 July 2020

Revised date: 14 September 2020

Accepted date: 14 September 2020

Please cite this article as: M. Kirchmeyer, F. Servais, A. Ginolhac, et al., Systematic Transcriptional Profiling of Responses to STAT1- and STAT3-Activating Cytokines in Different Cancer Types, *Journal of Molecular Biology* (2020), https://doi.org/10.1016/j.jmb.2020.09.011

Systematic transcriptional profiling of responses to STAT1- and STAT3-activating cytokines in different cancer types

Mélanie Kirchmeyer[1+], Florence Servais[1+], Aurélien Ginolhac[1], Petr V. Nazarov[2], Christiane Margue[1], Demetra Philippidou[1], Nathalie Nicot[2], Iris Behrmann[1], Claude Haan[1+], Stephanie Kreis[1+*].

[1] Signal Transduction Laboratory, Department of Life Sciences and Medicine, University of Luxembourg, 6 Avenue du Swing, L-4367 Belvaux, Luxembourg.

[2] Quantitative Biology Unit, Luxembourg Institute of Health, 1A-B rue Thomas Edison, L-1445 Strassen, Luxembourg.

[+] equal contributions

*To whom correspondence should be addressed.

Corresponding author: Stephanie Kreis (Assistant Professor). Department of Life Sciences and Medicine (DLSM). University of Luxembourg. 6, Avenue du Swing, L-4367 Belvaux, Luxembourg. Phone: +352 466644 6884. Fax: +352 466644 6435

Running title: Cytokine-induced transcriptomic responses in cancer cells

Keywords: Transcriptome, signaling, cytokines, cancer, profiling, melanoma, colorectal cancer, hepatocellular carcinoma

Declarations:

- **Ethics approval and consent to participate**: Not applicable
- **Availability of data and material**: The datasets generated during and/or analyzed during the current study are available in ArrayExpress under accession number E-MTAB-6080 and E-MTAB-9118, respectively
- **Competing interests**: The authors declare no competing interests

- Word count: 6232; Total number of figures and tables: 6, Additional files: 10

Abstract

Cytokines orchestrate responses to pathogens and in inflammatory processes but they also play an important role in cancer by shaping the expression levels of cytokine response genes. Here, we conducted a large profiling study comparing miRNome and mRNA transcriptome data generated following different cytokine stimulations. Transcriptomic responses to STAT1- (IFNγ, IL-27) and STAT3-activating cytokines (IL6, OSM) were systematically compared in nine cancerous and non-neoplastic cell lines of different tissue origins (skin, liver and colon).

The largest variation in our datasets was seen between cell lines of the three different tissues rather than stimuli. Notably, the variability in miRNome datasets was a lot more pronounced than in mRNA data. Our data also revealed that cells of skin, liver and colon tissues respond very differently to cytokines and that the cell signaling networks activated or silenced in response to STAT1- or STAT3-activating cytokines are specific to the tissue and the type of cytokine. However, globally, STAT1-activating cytokines had stronger effects than STAT3 inducing cytokines with most significant responses in liver cells, showing more genes up-regulated and with higher fold change. A more detailed analysis of gene regulations upon cytokine stimulation in these cells provided insights into STAT1- versus STAT3-driven processes in hepatocarcinogenesis. Finally, independent component analysis revealed interconnected transcriptional networks distinct between cancer cells and their healthy counterparts.

Introduction

The transcriptome is a highly dynamic assembly of different RNA molecules that either code for protein (mRNAs), have structural functions (such as tRNAs, rRNAs, snoRNAs) or are involved in gene regulation (such as miRNAs, lncRNAs). High-throughput transcriptome profiling can therefore provide information on cell type characteristics and cellular states including insights into which signaling and regulatory pathways are active [1-3]. A plethora of transcriptomic profiles of different cell types, in diseases and at different developmental stages are publically available. With the aim to pinpoint gene expression changes to specific tissues or cancers and to improve tailored drug treatment, the so-called NCI-60 study was the first milestone study analyzing 60 cancer cell lines derived from more than 10 tissues (such as skin, breast, prostate, lung) [4]. Since then, specific changes in gene expression of many cancers were successfully used to define sub types and to predict response to drugs and overall survival [5, 6].

The ongoing and rapid development of improved technologies allowing for high throughput profiling of transcriptome changes has fueled large and searchable data collections such as the TCGA (The Cancer Genome Atlas, https://www.cancer.gov/tcga), the Expression Atlas (https://www.ebi.ac.uk/gxa/home), the Gene Expression Omnibus (GEO, https://www.ncbi.nlm.nih.gov/geo/), CCLE (https://portals.broadinstitute.org/ccle) and many others. The ENCODE initiative (Encyclopedia Of DNA Elements) has funneled the enormous amounts of diverse data into well-organised databases with clear technical and quality control guidelines for data generation, curation and analysis (https://www.encodeproject.org/data-standards/).

Cytokines are involved in many fundamental biological processes [7, 8]. They mainly act via Janus kinases (Jaks), which trigger tyrosine-phosphorylation of STAT transcription factors, 7 of which exist in humans [9]. The importance of cytokine-induced processes in maintenance and spreading of tumors is undisputed [10]. Interestingly, STAT1 and STAT3 can have opposing roles in tumorigenesis: STAT3 promotes tumor cell growth and survival, proliferation, cell migration, angiogenesis, and inhibits apoptosis while STAT1 is involved in antiviral and immune defense, promotion of apoptosis and inhibition of angiogenesis and proliferation [11]. In this context, tumors can lose sensitivity to the IFNγ/STAT1 pathway and thus become resistant to the direct anti-proliferative and pro-apoptotic effects of IFNγ [12].

MicroRNAs (miRNAs) are non-coding RNAs produced by a multistep biogenesis pathway, which generally down-regulate gene expression of specific target mRNAs. Their profound regulatory effects and their central role in diverse cellular and developmental processes have led to the hypothesis that dynamic expression changes of miRNAs contribute to human disease, including cancer [13, 14].

Recent studies by our group and others have identified several miRNAs to be induced by cytokine stimulation and to play an important role in processes involved in cancer development and maintenance as well as resistance to drugs [15-20]. One of the first reports to demonstrate miRNA regulation following cytokine stimulation was undertaken in multiple myeloma cells, where miR-21 was up-regulated in a STAT3-dependent manner in response to IL6 [21]. In the following, miR-21 was shown to be increased by STAT3 in various tumor cell lines (prostate cancer cells, B16 melanoma cells) promoting proliferation, migration and survival in metastatic tumors [22-24]. The multi-faceted regulatory influence of miRNAs on cell homeostasis and the many roles of miRNAs in carcinogenesis have been well documented [13, 25, 26] .

Previously, we have shown [17] that IFNγ leads to a strong regulation of the miRNome in A375 melanoma cells. Surprisingly, when a similar experiment was performed in hepatoma cells stimulated with hyper-IL6 (HIL6, a "designer cytokine" comprising IL6 bound to the extracellular domain of IL6Rα), we observed almost no regulation at the miRNA level. On the other hand, primary healthy liver cells stimulated with IL6 showed many robust transcriptomic changes [15]. This led us to conduct a larger analysis in order to (i) understand the inter-tissue variations of the whole transcriptome and miRNome in skin, colon and liver, (ii) the differences between cancerous and non-neoplastic cells, and (iii) to define the impact of STAT1- (IFNγ and IL27) and STAT3-activating (HIL6 and OSM) cytokines on gene regulatory networks in the different cell lines. We identified interesting new and cell type-specific miRNA and mRNA responses to cytokine stimulations and confirmed several previously described transcriptomic regulations. Most profound changes were scored in liver cells when STAT1- and STAT3-inducing cytokine programs were compared: the regulated pathways are implicated in key cellular processes like apoptosis and immune responses.

Materials and Methods

Cell culture and cytokine stimulation

Cells were grown at 37°C in a water-saturated atmosphere at 5% CO_2 and in culture media as outlined in **Supplementary Figure 1.** Further details are given in **Supplementary Figure 1B** and as described before [15, 19].

Four cytokines were used for stimulations at previously established saturating concentrations: two STAT1-activating cytokines, interferon gamma (IFNγ, 50 ng/mL, Peprotech) and recombinant human interleukin-27 (rhIL27, 50 ng/mL, R&D systems) and two STAT3-activating cytokines, hyper-IL6 (HIL6, 20 ng/mL, a kind gift of Prof. Stefan Rose-John, University of Kiel, Germany) and Oncostatin M (OSM,

20 ng/mL, Peprotech). Cells were seeded at day 1 and stimulations were done for 3, 12, 24, 48 and 72 hours. For following western blot analysis and RNA extraction, cells were harvested all together at the end of the experiment. All cell lines were regularly checked to be mycoplasma-free and were either purchased shortly before the experiments or authenticated shortly before or after use in this study (DSMZ, Germany).

RNA extraction

Total RNA from cell lines was isolated using Quick-RNA MiniPrep Kits (Zymo Research) with an additional in-column DNase I treatment. Purity and quantity of RNA samples were assessed using a NanoDrop ND-2000c spectrophotometer (Thermo Scientific) and an Agilent Bioanalyzer 2100 (Agilent Technologies).

Microarray analysis

Microarray experiments were performed in collaboration with the Quantitative Biology Unit at the Luxembourg Institute of Health (Strassen, Luxembourg). Extracted total RNA of duplicate (stimulated) or triplicate (unstimulated) samples were used (with the exception of three additional independent replicates for unstimulated PH5CH8 cells, as the IL27 stimulation had to be re-done in another experiment) for downstream microarray studies using Affymetrix GeneChip miRNA 3.0 Arrays (based on miRBase version 17) and Affymetrix GeneChip Human Transcriptome Array (HTA) 2.0 according to the manufacturer's instructions. For mRNA arrays, 24h treatment samples were used; for miRNA arrays, 72h treatment samples were used as this turned out to be the best time point to analyze miRNA regulation [17], next to untreated controls. The microarray data were pre-processed, quality was controlled and a filtering step of lowly abundant genes was performed as before [31]. All genes that were below a defined threshold of 5 in $\log_2$ scale were removed, which increased the number of significantly regulated genes for each cell line with treatment. Before statistical analysis of mRNA data, Affymetrix features – transcript clusters were summarized at gene level. For miRNA arrays, only mature human miRNAs were considered. Microarray data are summarized in **Supplementary Table 1**.

Data and material availability: mRNA and miRNA datasets are available under accession number E-MTAB-6080 and E-MTAB-9118, respectively.

Western blots

To confirm successful cytokine stimulations, cells were seeded and stimulated in parallel to the cells for microarray experiments. Cell lysis was performed as described before [19]. The following antibodies were used: phospho-STAT1 (1:1000, BD Biosciences Cat# 612233, RRID:AB_399556),

STAT1 (1:1000, BD Biosciences Cat# 610116, RRID:AB_397522), phospho-STAT3 (1:1000, Cell Signaling Technology Cat# 9145S, RRID:AB_561305), STAT3 (1:1000, BD Biosciences Cat# 610190, RRID:AB_397589) or α-tubulin (1:5000, Santa Cruz Biotechnology Cat# sc-32293, RRID:AB_628412). The HRP-conjugated secondary antibodies were purchased from Cell Signaling Technologies. Antibody complexes were detected by using enhanced chemiluminescence (ECL) technology [27] on a Fusion FX (Vilber) CCD camera system.

Flow cytometry

Cells were resuspended in cold PBS supplemented with 5% FBS and 0.1% sodium azide and incubated with a mouse antibody specific for OSM-R (200µg/mL, Santa Cruz) or the corresponding IgG control antibody (1µg/µL, Immunotools) for 1h at 4°C. After washing, cells were incubated with a secondary antibody against mouse IgG coupled with R-phycoerythrin (1:100, Jackson) for 1h at 4°C and analyzed on a FACSCanto II flow cytometer using FACSDiva (BD Biosciences) software. Overlays were created using the FlowJo software.

Principal and Independent Component Analyses (PCA, ICA)

Microarray data of cell lines responding to the 4 cytokine treatments (PH5CH8, Hep3B, Huh7, NHEM, A375, MelJuso, NCM460, HCT116 and HT29) were subjected to PCA. Computation and plotting were performed using R (v3.4.0) and Rstudio (v1.1). The PCA was computed using the R package FactoMineR (v1.36) [28] and plotted on the R package factoextra (v1.0.4) [29]. Other plots were generated using the R package ggplot2 (v2.1) [30] and the collection of packages tidyverse (v1.1) [31]. All experiments were scaled to the same unit, as the IFNγ stimulation for NHEM cells possessed a larger variance compared to the other experiments.

Consensus independent component analysis (ICA) was performed by the consICA tool as previously described [32], with the core computation performed using R package fastICA (v1.2-2). The method decomposes the expression matrix into statistically independent signals (or components) in the space of genes and their weights in the space of samples. These signals can be associated with cell types and biological processes within cells. ICA was performed using 20 components which were associated to biological processes by GO enrichment analysis using package topGO (v2.38.1) and to experimental conditions using ANOVA.

Correlation analysis of mRNA and miRNA as well as comparison to TargetScan predictions was performed by CoExpress tool [33].

Analysis of publically available datasets from the TCGA initiative

mRNA and miRNA expression data were extracted from TCGA cohorts with UCSC Xena browser. For mRNA gene expression, RNAseq (PolyA + Illumina pancan normalized) data and for miRNA, miRNA gene expression (IlluminaHiseq) data were used to validate the results. Only patients with matching pairs (Solid Tissue Normal and Primary Tumor samples) from TCGA Bladder Cancer (BLCA), TCGA Breast Cancer (BRCA), TCGA Colon Cancer (COAD), TCGA Colorectal Cancer (COADREAD), TCGA Esophageal Cancer (ESCA), TCGA Head and Neck Cancer (HNSC), TCGA Liver Cancer (LIHC), TCGA Lung Cancer (LUNG), TCGA Prostate Cancer (PRAD) and TCGA Stomach Cancer (STAD) cohorts were considered for the analysis with, respectively, 19, 75, 26, 30, 11, 43, 50, 109, 52 and 32 matched pairs.

Statistical analysis

Matching solid tissue normal and primary tumor samples from various TCGA cohorts were compared to each other with Wilcoxon matched-pairs signed rank test in GraphPad Prism v7.03 software. Differential expression analysis was performed using R package limma (v.3.42).

Results

Characteristics of analyzed transcriptomes and miRNomes

We have performed and analyzed a total of 186 microarrays, 88 mRNA and 98 miRNA arrays, derived from 9 cancerous and non-neoplastic cells lines representing 3 different tissues, stimulated with 4 distinct STAT-activating cytokines. A graphical overview of the study and details of cell lines are shown in **Supplementary Figure 1**. Each cell line was cultured in cell type-specific media allowing for optimal growth (**Supplementary Figure 1B**). Different media compositions might influence the expression of genes and miRNAs when comparing cell lines with each other, however, these effects are expected to be marginal. Expression of selected cell type-specific transcription factors (**Supplementary Figure 1C)** further indicated the authenticity of cell lines. Interestingly, the primary liver cells PH5CH8 showed expression patterns very similar to melanoma cells for key transcription factors MITF, HNF1A, HNF4A and CDX2 suggesting overall similar gene and miRNA expression profiles between these cells, which turned out to be the case.

Optimal time points for measuring mRNA and miRNA responses following cytokine treatments had been established before for melanoma cells [17, 33] and by additional pre-tests for other cell lines (data not shown). In general, miRNA responses peak after mRNA responses and are best analyzed at 72h while mRNAs were profiled after 24h, in order not to miss too many of the early cytokine-

induced signals. Before microarray analyses, successful cytokine stimulation was ensured by detection of phosphorylation levels of phospho-Tyr^{701}-STAT1 following stimulation with IFNγ and IL27 and phospho-Tyr^{705}-STAT3 following HIL6 and OSM stimulation (**Supplementary Figure 2A**). Three cell lines (Hep3B, HT29 and NCM460) did not to react to OSM and their lack of the OSM-specific receptor (OSM-R) was confirmed by FACS analysis (**Supplementary Figure 2B**). Therefore, microarray analyses for OSM stimulations of these cells were not performed. Pearson correlation (**Figure 1C**) showed a correlation coefficient of mRNA arrays greater than 0.8 for the cell lines derived from the same tissue (skin in the bottom left corner, liver in the center and colon in the upper right corner). Surprisingly, PH5CH8 cells (non-neoplastic liver cells) clustered with colon-derived cells with which they correlated at more than 0.85, especially with cancerous colonocytes (HT29 and HCT116). Overall, and in comparison to miRNAs (**Figure 1**), mRNA expression profiles were more robust with less variability between replicates and among the same tissues. PH5CH8 cells also seemed to be different from HCC cell lines in the miRNA arrays and clustered here with skin-derived cells. Venn diagrams indicate the number of tissue-specific mRNAs/miRNAs (**Figure 1C**).

For a first overview of the microarray data, we performed Principal Component Analysis (PCA) (**Figure 1**). One unstimulated sample (Hep3B.Untreated.Hep3B_0) was marked as an outlier as the profile for this sample was incoherent with the two other replicates (Hep3B.Untreated.Hep3B_1 and _2) and was removed from following analyses. In the PCA, the cancer cell lines of each tissue were separated from the non-cancer cells while cytokine stimulation had little effect. This was visible at the mRNA (**Figure 1A**) and at the miRNA level (**Figure 1B**) although less pronounced for miRNAs. On mRNA level (**Figure 1A**), all samples from a given tissue clustered closely together, with the exception of PH5CH8 cells. Next, hierarchical clustering analysis revealed two main groups for mRNAs (**Figure 1A**). The first cluster contained the three skin-derived cell lines (yellow) and PH5CH8 cells. All other liver- and colon-derived cells formed a second group. Again, miRNA heatmaps underline the higher variability in miRNA levels and show that the 2 healthy lines, NHEM and PH5CH8, do not group within their respective tissues (**Figure 1B**). Overall, samples from a particular cell line consistently grouped together irrespective of cytokine treatment indicating that the difference between cell lines was clearly greater than the transcriptomic changes induced by stimulation with cytokines, even within the same tissue.

With an overall detection threshold of $\log_2 > 5$ (see Material and Methods), we found that 19803 (61%) features (from 32670 present on HTA arrays) were expressed in at least one sample. These features corresponded to 18635 annotated genes. Among 12867 non-expressed features, 6960 (54%) were composed of predicted genes, pseudogenes and non-coding genes. For miRNAs, 1294 of 1733 mature human miRNAs were absent in all 9 cell lines, leaving only 439(25%) of the miRNome expressed. A summary of feature numbers for mRNA and miRNA arrays is provided in

Supplementary Figure 3. Some miRNA gene families showed a tissue-dependent or a cell-specific expression: the miR-200 family members were exclusively detected in colon cells, miR-122 was specific for liver, miR-152 specific for skin while the 17 miRNAs of the let-7 family were absent from cancerous liver cell lines (data not shown). Cell type-specific miRNAs were mainly enriched in 2 tissues: epithelial cells for colon cell lines (FDR=2.5e-3) and hepatocytes for liver cell lines (FDR=2.0e-2) (**Supplementary Table 2A**).

In order to identify inversely correlated miRNAs/mRNAs in our dataset, which could be indicative of a functional connection, we used the CoExpress software (http://sablab.net/coexpress.html) [33]. With a high confidence threshold of absolute Pearson correlation > 0.925, we found 11 miRNAs inversely correlated with mRNAs (**Supplementary Table 2B**) that were also predicted, albeit with generally low scores, by TargetScan. Inverse correlation of miRNAs and mRNAs from public or own data sets can be a useful additional parameter to improve target gene predictions. Furthermore, correlated expression of intronic miRNAs together with their "host genes" was found for several pairs such as miR-107/PANK1, miR-139/PDE2A, miR-149/GPR1, miR-208/MYH6, miR-211/TRPM1, miR-326/ARB1, miR-342/EVL, and miR-346/GR1D1 (data not shown). These co-regulations are interesting and their regulatory potential is not yet fully understood as intronic miRNA expression levels vary with up- or down-regulation of their vehicle genes. When the host gene is specifically up-regulated during oncogenic transformation, tissue damage or in response to stimuli such as cytokines, the intronic miRNA levels also increase, which might have a negative impact on the respective miRNA target genes.

To illustrate relationships and possible interactions between mRNAs and miRNAs across the entire data set, we used independent component analysis (ICA), which we recently applied to large transcriptomic data sets of melanoma cells [32].

Tissue-and cancer-specific miRNA and mRNA expression

Next, we analyzed the tissue-specific expression of miRNAs and mRNAs. Features were selected in the following way. First, mean expression was calculated for replicates in each sample group for each cell line with and without treatment. Next, a feature was called "stably expressed", if in one of the conditions the mean $\log_2$ expression was above 5. Averaging expression among replicates allowed reducing randomness of observation. Using this approach, we estimated 15163 stably expressed mRNAs and 260 miRNAs. Venn diagrams (**Figure 1C**) show that 604, 645 and 764 mRNAs were exclusively expressed in liver, colon, and skin, respectively. This corresponds to 4-5% of all herein stably detected mRNAs. Over 76% of mRNAs were expressed in all tissues. At the miRNA level, about 63% (165) of stably expressed miRNAs were commonly present in all tested tissues and these miRNAs were connected to general functions like cytoskeleton remodeling, apoptosis, survival or cell

cycle (data not shown). Ten, 18, and 17 specific miRNAs (**Figure 1C**) were found to be expressed in liver, colon, and skin, respectively. These low numbers rendered the building of networks or common pathways difficult. Therefore, we performed ICA analysis [32], which enables the identification of sources of transcriptional signals, clustering of genes into functional groups and cell type-related signatures [34] and the deduction of interactions between biological functions [35]. A global overview of all components representing miRNAs (MICs) and mRNAs (RICs) and their connections is shown in **Figure 2A**. The two components with the strongest connection between them (indicated by the thickness of the line) are highlighted: MIC7 and RIC12. A list of members of these components (inserted) contains interesting pairs that are known to interact (e.g. AXL and miR-34a [36, 37]) or are known target genes of cytokines (e.g. IFI6, IFI16). Interestingly, distinct MIC and RIC components were able to discriminate between tissues (**Figure 2B**).

In order to find cancer-specific mRNAs or miRNAs, we identified MIC and RIC components 1, which distinguished between cancer cells and their healthy counterparts with high stability (**Figure 3A).** Members in these components are involved in immune responses in general and in viral and IFNγ-induced immune responses in particular, indicating that these basic cellular responses are distinct in normal versus cancerous cells (**Supplementary Figure 4**)

Next, we generated a list of cancer-related genes for each tissue by comparing differentially expressed mRNAs and miRNAs (DEG, FDR (false discovery rate) ≤ 0.05) between each cancerous cell line and corresponding non-neoplastic cells. Considering mRNAs found in common between all cell lines and expressed with a $\log_2|FC|$ above 1 compared to healthy cells, 28 mRNAs were significantly regulated, however, only 1 mRNA was up-regulated in all cancerous cells (*FAM171B*) while 4 were down-regulated (**Figure 3B and C).** Although the other genes were not consistently up- or down-regulated, 2 interesting genes showed the same expression pattern in all but one cell line: *GTSF1* and *DNAJC15*. Altogether, we identified two mRNAs more abundant (*FAM171B* and *GTSF1*) and five less abundant (*FAM21B*, *FAM43A*, *OAS1*, *REPS2* and *DNAJC15*) in cancerous versus normal cells.

To extrapolate our findings to a broader range of cancer tissues, TCGA datasets from a panel of ten cancers (https://www.cancer.gov/tcga) were incorporated. As only data from matching pairs (Solid Tissue Normal and Primary Tumor) were considered, comparisons were performed on bladder (19 pairs), breast (75), colon (26), colorectal (30), esophageal (11), head and neck (43), liver (50), lung (109), prostate (52) and stomach (32) cancer cohorts (**Supplementary Figure 5**). Only few data from normal tissues were available for melanoma, pancreas and rectal cancer, so no comparison could be made for those cancers. *FAM171B* was clearly increased in liver and lung cancer cells (red circles), while it was reduced in breast and colorectal cells (blue circles). *GTSF1* had significantly higher expression levels in liver, breast and head and neck cancer cells compared to normal cells and inverse expression levels in colorectal cancer cells. *DNAJC15* was slightly less abundant in liver, lung and

prostate tumor cells. Overall, this analysis shows that specific genes can either be up- or down-regulated in cancer versus normal counterpart cells depending on the tissue of origin: 29 mRNAs (AUC=1) and 4 miRNAs (AUC≥0.9) could potentially serve as biomarkers to distinguish cancerous versus non-neoplastic cells. However, the microenvironment and tissue biology likely also determine in which way certain genes are regulated upon oncogenic transformation, suggesting that cancer type-specific biomarkers in form of mRNAs or miRNAs might be more robust thank global markers for cancer.

Cytokine-specific mRNAs and miRNAs

IFNγ, IL27, HIL6 and OSM are known to have different functions in tumor biology. We compared the miRNome and transcriptome regulations in all cell lines (stimulated versus unstimulated) in order to understand gene regulatory differences between cytokine stimuli in cancerous and non-neoplastic cells of different tissues.

To further investigate transcriptomic regulation, only mRNAs and miRNAs with an FDR < 0.05 and $\log_2|FC| \geq 1$ or 0.5, respectively, were considered as "significantly differentially expressed" (in comparison to the expression levels in the respective unstimulated samples) and used in the subsequent analyzes. Generally, only few miRNAs (less than 100) were robustly regulated following cytokine stimulation (differentially expressed miRNAs in skin: 97 upon IL27, 99 upon IFNγ, 69 upon OSM and 6 upon HIL6; in colon: 2 upon IL27, 47 upon IFNγ, 7 upon OSM and 6 upon HIL6; in liver: 4 upon IL27, 12 upon IFNγ, 26 upon OSM and 26 upon HIL6). The overall weakest cytokine responses were seen in colon cells where only IFNγ induced 47 gene regulations while the other cytokines had marginal effects (see numbers above). Among liver cells, Huh7 reacted well to IL6-type cytokines and IL27, with 26 and 10 miRNAs, respectively differentially expressed compared to unstimulated controls. Among skin cells, NHEM and A375 showed several interesting miRNA responses to OSM and IL27, while IFNγ evoked the largest number of differentially regulated miRNAs in A375 cells as we have previously seen [17]. Numbers of up- and down-regulated genes and miRNAs are summarized in **Supplementary Table 1**. Since mRNA responses to the applied cytokine treatments were much more numerous and overall stronger, we continued to analyze mRNAs in more detail focusing on genes, which were regulated in at least 2 different conditions (in total 472 genes).

To specifically identify STAT1-regulated genes following IFNγ /IL27 treatments versus STAT3-regulated genes following OSM/HIL6 stimulations, we performed PCA (**Figure 4A)**. Eight conditions, which had less than 10 differentially expressed genes (HCT116-HIL6 and -OSM, PH5CH8-HIL6, A375-HIL6 and -OSM, MelJuso-HIL6, -OSM and -IL27) were removed from analysis, as this lack of response affected the overall PCA. The percentage variance of the dataset contributed by the different dimensions of the PCA was 43.6 % for the first dimension and 13.5% for the second. Thus, the first

two dimensions of the PCA represented 57.1 % of the total variance of the dataset, containing most of the information related to cytokine stimulation. For most cell lines, the projection of the "combined effect" for the different cytokine treatments (represented by the length and direction of the arrows, with each arrow representing one cytokine treatment condition (e.g. Hep3B-IL27)), showed a good overlap for IL27 and IFNγ. The light blue and dark blue arrows depicting IL27 and IFNγ, respectively correlated well with the location of the blue ellipse, representing 0.95% of the quantile distribution of validated IFNγ-regulated genes [38]. The IL27 and IFNγ responses were very similar, with the combined effect lines having an almost identical orientation. In contrast, the red and orange arrows representing HIL6 and OSM, respectively, correlated much less with the location of the orange ellipse, containing validated IL6-type cytokine-regulated genes [38]. This highlights the fact that the STAT3 response is more heterogeneous throughout different cell types and that the genes present in our list of validated IL6-regulated genes do not necessarily reflect the whole spectrum of responses in our 3 tissue types [39] **(Figure 4A)**. An overview of the 77 differentially regulated genes is shown in **Figure 4B**.

Interestingly, the mRNA responses to IL6-type cytokines were most pronounced in liver cells (134 and 94 differentially expressed mRNAs following OSM and HIL6, respectively) while colon cells were much less sensitive to IL6-type cytokines (**Supplementary Table 1**); some miRNA expression levels changed in all cell types, but to a generally lower extent. Therefore, PCA on mRNAs was conducted with liver cells only (**Figure 5A**). Here, the percentage variance of the dataset added up to 71.3 % for the first two dimensions. Interestingly, the "combined effect" for the different cytokine treatments, represented by the direction of the arrows shown in red/orange for IL6-type cytokines (OSM and HIL6) and blue for IFNγ and IL27, shows almost orthogonal orientations (more or less 90°). This corresponds to the situation in which only few genes are co- or counter-regulated with comparable intensity upon signaling of IL6-type and interferon-type cytokines. The situation in which the "combined effect" would point into opposing directions would indicate inverse regulation of genes with comparable intensity, while a matching orientation would indicate co-regulation with comparable intensity. In PH5CH8 cells, the angle between IL6-type cytokines and interferon-type signaling is even higher than 90°, which reflects the fact that in these cells a slightly higher number of genes were inversely regulated by the two types of treatments (**Figure 5A**). A heatmap of the 115 differentially regulated genes in liver cells is shown in **Figure 5B**.

Gene regulation following IL6-type and IFN-type cytokine stimulation

Next, we investigated the regulation of individual genes following IL6- and IFNγ–type cytokine treatments in the two PCA analyzes described above. For this, we highlighted and identified those 77

(all cells; **Figure 4B**) and 115 (liver cells; **Figure 5B**) mRNAs, which were significantly differentially expressed compared to untreated cells and which showed a good projection of the genes in question ($cos^2 \geq 0.75$) meaning that they contributed most to the principal components in the 2 dimensions depicted in the PCAs. The genes annotated in blue or orange (in **Figures 4C** and **5C**) were the ones found in the lists of validated IFNγ- or IL6-type-cytokine-regulated genes respectively [38], while the genes annotated in black were absent from these lists. In **Figure 4C** and **Figure 5C** many of the validated IFNγ target genes can be found to be indeed efficiently regulated by IFNγ and IL27. Thus, the IL27 and IFNγ transcriptomic responses were robust and conserved throughout cell lines and cell types and included genes involved in antiviral responses, antigen presentation, apoptosis and growth (see discussion). On the other hand, fewer of the validated IL6 targets were up-regulated upon HIL6 or OSM treatment in our cell lines (**Figure 4C)**, again reflecting the heterogeneity of the IL6/STAT3 response in different tissue types [39]. A higher number of validated IL6 targets were up-regulated upon HIL6 or OSM in liver cells (**Figure 5C**) indicating that the IL6/STAT3 response is strong in liver tissue.

To gain insights into cellular functions activated by IL6- or IFN-type cytokines, we performed a gene set enrichment analysis (GSEA, **Supplementary Figure 6**). As expected, various immune response functions were the overarching and top scoring cellular programs induced by cytokine stimulation, irrespective of the cell type. In addition to a subset of genes regulated effectively by both IL6-type and IFNγ-type signaling (e.g. complement factors) it was also evident that many of the differentially expressed genes were regulated by both the IFNγ-type (STAT1) and the IL6-type cytokines (STAT3) (**Figures 4** and **5**) although being efficiently regulated by one and less by the other factor. Since one of our aims was to specifically discriminate between the IFN type-mediated anti-cancer response (mainly STAT1-mediated) and the IL6-type pro-cancerous responses (mainly STAT3-mediated), we used this dataset and previous data to generate lists of genes regulated by only one type of treatment as well as genes counter-regulated by the two treatments (**Supplementary Figure 7** and **Supplementary Table 3**). This will also allow for a better discrimination between the two types of treatments in future studies.

Discussion

Many comparative data sets on transcriptomic profiling are available in online repositories. However, a systematic and meaningful comparison is often hampered by technical variations, platforms, cells and experimental conditions between the data of interest. Here, we conducted a large profiling study

ensuring high reproducibility and comparability between data. We have generated a total of 186 data sets encompassing whole miRNome and transcriptome (mRNA) data from 9 cell lines derived from 3 tissues, representing cancerous and healthy counterparts, stimulated or not with 4 different cytokines (IFNγ, IL27, HIL6 and OSM).

In Pearson correlation heatmaps for mRNAs and miRNAs (**Figure 1C**), samples from the same cell line clustered together rather than by treatment indicating that cell-specificities had more impact than differences induced by stimulation with cytokine, even within the same tissue. However, if only top-regulated genes were considered, IFNγ- and IL27-stimulated samples were grouped closer together than cell lines, which was not the case for HIL6 or OSM-stimulated samples. This suggests a stronger and a more general, cell type-independent gene regulation by STAT1-activating cytokines compared to STAT3-activating cytokines, which may be explained by the wide role of interferon/STAT1 in innate immunity and antiviral defense.

Overall, mRNA expression profiles seemed to be more accurate in defining tissue origin than miRNA expression. To further characterize tissue-specificity, gene expression comparisons were performed on all unstimulated samples. For mRNA, more than 85% of expressed genes were commonly present in all tested cell lines and associated with the basal activity of a cell, including metabolic or biosynthesis processes, biological regulation or cell communication. More than 500 genes, mainly involved in metabolic process, were exclusively expressed in colonocytes while melanocytes expressed 686 genes involved, for example, in cell-cell adhesion or neurogenesis. Hepatocytes, on the other hand, specifically expressed about 400 genes involved in processes attributed to general liver functions similar to what has been described before[1, 40].

In the three cancer types analyzed here, only two genes were consistently up-regulated in cancer cells versus their healthy counterparts: FAM171B and GTSF1 (**Figure 3C**). Interestingly, GTSF1 (Gametocyte Specific Factor 1) has been suggested, upon knock-out in male mice, to prevent apoptosis [41]. In melanoma, breast, head and neck, liver, and colorectal cancer, GSTF1 was significantly increased (**Figure 3 and Supplementary Figure 5**) and has recently been put forward as a diagnostic biomarker for cutaneous T-cell lymphoma [42].

The product of a consistently down-regulated gene, DNAJC15 (DnaJ Heat Shock Protein Family (Hsp40) Member C15) is anchored in the mitochondria inner membrane and involved in the regulation of the respiratory chain [43] and apoptosis [44]. Additionally, its expression has been associated with enhanced drug sensitivity in ovarian [45] and breast [46] cancers. We found DNAJC15 significantly down-regulated in melanoma, liver, lung, prostate, and colon cancer (**Figure 3C, Supplementary Figure 5**). Overall, the large number of studies looking for prognostic or diagnostic biomarkers in form of mRNAs and miRNAs for cancer in general and for specific cancers in particular, have so far not yielded the initially expected success. Also here, no robust candidate was found that

would show an up- or down-regulation high enough to be considered as a promising specific biomarker.

In our study, the cytokine-specific transcriptomic responses turned out to be more rewarding. The IL27 and IFNγ transcriptomic responses were robust and conserved throughout cell lines and cell types while HIL6 or OSM stimulation induced a quite diverse response in the cell lines we investigated. A closer inspection of the differentially regulated genes in liver cells (PH5CH8, Huh7 and Hep3B) showed that IFNγ and IL27 efficiently and specifically up-regulate genes involved in antiviral defence, a mechanism that is highly conserved in all cell types, involving genes regulating direct antiviral processes, antigen presentation, immune escape, apoptosis and growth. Evidently, most of these processes involved in antiviral defence are also crucial processes in the interferon-mediated anti-cancer response, as discussed below (see also **Figure 6** for an overview). One subset of genes regulated efficiently by both IFNγ-type and IL6-type cytokines in liver cells were complement factors such as C1R, C1S, C2, C3, C4B, CFB and additionally ICAM1 and TGM2 (**Figure 5B** and **C**).

IFNγ and IL27 regulate genes involved in interferon-type signalling itself, such as STAT1, STAT2, IRF1 and NMI, all of which positively regulate the interferon-type signalling. IRF1 and STAT1 are crucial transcription factors regulating IFNγ and IL27 responses and NMI is known to enhance STAT1-dependent effects. IFNγ and IL27 (through their activation of STAT1) are considered to have anti-cancer activity while IL6 and OSM (through their activation of STAT3) are thought to have tumor promoting functions. The anti-cancer and pro-cancer activities of STAT1 and STAT3, respectively are regulated first by the level of phosphorylated STATs found in cancer cells and secondly by the level of protein expression of the individual STATs and thus by the ratio of STAT1 versus STAT3 [11, 47]. Thus, a higher ratio of STAT1 versus STAT3 protein levels (such as the one induced here by IFNγ and IL27) influences the pro-cancer activities of STAT3 negatively (reviewed in [48]).

Secondly, upon IFNγ and IL27 stimulation, we found an up-regulation of mRNAs of genes coding for proteasomal subunits (PSMB 8/9/10, PSME2, PSME2P2), other proteases (ERAP1, CTSS, Lap3), HLA subunits (HLA-B, -C, -E, -H, BTN3A1-3), TAP transporters (Tap1, Tap2) which are involved in the presentation of cancer antigens by the cancer cell [49] (**Figure 5B** and **C, Figure 6**). PD-L1 (CD274), which we found to be specifically up-regulated by IFNγ and IL27 is well known to be involved in immune tolerance in many cancer cell types [38] (**Figure 5B** and **C, Figure 6**). In addition, the chemokine CXCL10, associated with chemotaxis of cells associated with a T_H1 response and the suppression of angiogenesis, was also specifically up-regulated by IFNγ and IL27 [48]. Finally, IFNγ and IL27 also efficiently regulated genes involved in apoptosis (such as ApoL6, IFI6, MLKL, TNFSF10, TNFRSF10D) and cell growth (RARRES3, considered a tumor suppressor).

In liver cells, IL6-type cytokines (HIL6, OSM) expectedly up-regulated acute phase proteins like SPINK1, SERPINA3, SAA4, MBL2, LBP, IL1R1. Additionally, also genes of the IL6-type signalling pathway itself were induced such as the negative feedback regulator SOCS3 or the OSM receptor (OSMR). Interestingly, IL6-type cytokines also regulated the chemokines CXCL2 and CXCL5, which both recruit neutrophils to sites of inflammation or tumors. Other factors from the TME (tumor microenvironment) induce neutrophils to release high levels of angiogenic factors (e.g. TGFβ, IL8, VEGF) and to directly or indirectly lead to the release of immunosuppressive cytokines (e.g. TGFβ, IL10, IL6) (**Figure 5B** and **C, Figure 6**) (reviewed in [50]).

IL6 is also known to promote metastasis in HCC[2, 51]. For example, LRG1, shown to be upregulated upon stimulation with IL6-type cytokines (**Figure 5B and C**) and involved in a switch in TGFβ signaling, is potentially involved in metastasis. LRG1 binds to TGFβ receptors and co-receptors promoting the use of the TGFβRII/ALK1/SMAD1/5/8 pathway, which in turn mediates angiogenesis and metastasis [52]. Interestingly, EFNA1 up-regulation by the IL6-type cytokines is also associated with increased angiogenesis. Other IL6-type cytokine-regulated genes found in our data set involved in metastasis are BHLHE40 and LINC00941 which both promote metastasis and growth (**Figure 5B** and **C, Figure 6**) [53, 54].

Altogether, our conclusions from the liver cell analysis support the different functions of IFNγ-type/STAT1 and IL6-type/STAT3 signaling in cancer. The IL27 and IFNγ transcriptomic responses are robust and conserved across various cell types, having mostly anti-cancer functions (growth reduction, apoptosis, antigen presentation, inhibition of angiogenesis). On the other hand, HIL6 and OSM stimulation up-regulate pro-angiogenic and -metastatic genes as well as chemokines that trigger tumor-associated neutrophils to produce immunosuppressive cytokines **(Figure 6**). Apart from confirming previously described response genes of STAT1 and STAT3, we identified a more specific set of genes that have defined roles in the physiology of healthy liver cells as well as in hepatocellular carcinoma. Overall, and in contrast to the robust regulation seen at the mRNA level upon cytokine stimulation, miRNome responses were much more variable and weaker with few miRNAs differentially regulated following stimulation with the herein investigated cytokines (**Supplementary Table 2**). Finally, the analysis and integration of miRNome and transcriptome data sets by ICA, respectively revealed components, i.e. groups of mRNAs and miRNAs that together identify biological functions that would be missed when analyzing either data set alone.

Solid tumors are embedded in their tissue of origin surrounded by cells of the microenvironment (fibroblasts, endothelial cells, immune cells and others). Types and amounts of cytokines, chemokines and growth factors secreted by such cells have an impact on the development and

progression of the tumor. Here, we quantified gene regulatory events on a global scale to provide insights into anti- or pro-cancerous cellular programs that are stimulated or silenced by comparing the impact of STAT1 versus STAT3- activating cytokines on healthy cells and cancer cells of three different tissues. Interestingly and overall, skin and colon-derived cancer cells reacted weaker to cytokine stimulations with relatively few target gene networks being turned on compared to hepatocellular carcinoma cells, which revealed robust new and known STAT target genes. In sum, IL6/OSM>STAT3-activated cellular programs led to angiogenesis and metastasis whereas IFN-Y/IL27>STAT1 had opposing effects resulting in cell death, growth arrest and increased immunogenicity against the tumor cells.

Acknowledgements

We thank Prof. Dr. Stefan Rose-John (University of Kiel, Germany) for providing hyper-IL6 (HIL6). We thank our collaborator Prof. Dr. Nobuyuki Kato (Department of Molecular Biology, Okayama University, Japan) for providing the PH5CH8 cells and Dr. Elisabeth Letellier for providing colon cancer cells.

This work was funded by the Luxembourg National Research Fund (FNR) and the Deutsche Forschungsgemeinschaft (C12/BM/3975037, Inter project "HepmiRSTAT"), by the Internal Research Project «IL6LongLiv» of the University of Luxembourg and by the Cancer Luxembourg (SecMelPro grant), and by Luxembourg National Research Fund (C17/BM/11664971, CORE project DEMICS).

Figure legends

Figure 1: Global overview of transcriptome and miRNome data sets. Principal Component Analysis (left) and heatmap (right) of mRNAs (**A)** and miRNAs **(B)** of colon- (blue), liver- (green) and skin-derived (yellow) cells upon cytokine stimulation. Heatmaps show unsupervised hierarchical clustering

of the 472 mRNAs differentially expressed upon 72h of cytokine stimulation (HIL6, OSM, IFNγ and IL27) in colon- (HCT116, HT29 and NCM460), liver- (Hep3B, Huh-7 and PH5CH8) and skin-derived cells (A375, MelJuso and NHEM). **(C)** Pearson correlation of all microarray data sets. Global unsupervised correlation analysis for mRNAs and miRNAs of cell lines as described in (B). Venn diagrams indicate numbers of expressed mRNAs and miRNAs in tissues (regardless of stimulation).

Figure 2: ICA analysis of miRNome and transcriptome data sets of all cell lines. (A) Correlated mRNA and miRNA components (RICs and MICs) detected by consensus ICA. Edges connect components with $R^2 > 0.5$. Colors of edges corresponds to positive (red) or negative (blue) correlations. **(B)** Some RICs and MICs show specificity for different organs. The weights of RIC3, RIC4, RIC5, MIC3, MIC4 and MIC12 show specific behavior for cell lines originated from colon, liver and skin. ANOVA p-values are reported for each violin plot.

Figure 3: Discriminating cancer from healthy cells. (A) ICA component 1 for both RNAs (RIC1) and miRNAs (MIC1) distinguish healthy from cancer cells across the three different cell types. **(B)** Table of significant, up- and down-regulated mRNAs ($\log2|FC| > 1$) compared to the respective non-neoplastic cell line (FDR < 0.05) in unstimulated colon-, liver- and skin-derived cells compared to the other cell lines. **(C)** Expression levels and functions of the most significantly up- and down-regulated mRNAs in cancerous versus non-neoplastic cells (red: up-regulated; grey: down-regulated). Full names of genes are given in the main text.

Figure 4: Global responses of all investigated cells to different cytokines. (A) PCA analysis of the differentially expressed mRNAs (FDR < 0.05 and $\log_2|FC| \geq 1$) for all cell lines and for treatments eliciting a response of > 25 mRNA regulated (therefore less data derived from HIL6/OSM stimulations are included). The light blue and dark blue arrows representing IL27 and IFNγ, respectively, correlate quite well with the location of the blue ellipse, which represents the 0.95% quantile distribution of validated STAT1 genes. **(B)** The heatmap shows genes differentially regulated compared to unstimulated controls considering the following thresholds: FDR < 0.05, $\log_2|FC| \geq 1$ and $\cos^2 \geq 0.75$. **(C)** PCA using the same thresholds as in B. Individual genes are annotated. Their presence in the lists used for ellipse construction is highlighted by a color code.

Figure 5: Specific responses of liver cells to different cytokines. (A) PCA analysis of the differentially expressed mRNAs (FDR < 0.05 and $\log_2|FC| \geq 1$) for treatments eliciting a response of $>$ 25 mRNA regulated in liver cell lines. The light blue and dark blue arrows representing IL27 and IFNγ

respectively correlate quite well with the location of the blue ellipse, which represents the 0.95% quantile distribution of validated STAT1 genes. **(B)** The heatmap shows genes differentially regulated compared to unstimulated conditions considering the following thresholds: FDR < 0.05, $\log_2|FC| \geq 1$ and $\cos^2 \geq 0.75$. **(C)** PCA using the same thresholds as in B. Individual genes are annotated. Their presence in the lists used for ellipse construction is highlighted by a color code.

Figure 6: Schematic representation of the cytokine signaling pathways and important regulated genes and functions supported by these genes. The different cytokine receptor complexes are shown alongside distinct responses elicited by the IFNγ-type (STAT1) and IL6-type (STAT3) signaling shown either in green (anti-tumor response) or red (pro-tumor response) writing and arrows. The genes we found specifically regulated are shown in black writing.

Supplementary Files

Supplementary Table 1. Number of differentially expressed mRNAs and miRNAs. Differentially expressed mRNAs (A) and miRNAs (B) in liver-, colon-, and skin-derived cells stimulated with IL27, IFNγ, OSM or HIL6 in comparison to unstimulated control cells. Thresholds: FDR < 0.05, $\log_2|FC| \geq 0.5$ (miRNAs) and $\log_2|FC| \geq 1$ (mRNAs).

Supplementary Figure 1. Schematic study overview. (A) Scheme illustrating the study design and **(B)** Details on used cell lines. **(C)** $\log_2$ expression of a selection of tissue-specific transcription factors is shown for different cell lines.

Supplementary Figure 2. Control experiments of cytokine stimulations. (A) Western blot analysis for validation of successful cytokine stimulations in colon-, liver- and skin-derived cells. **(B)** FACS analysis confirming absence of OSMR expression in selected cell lines. Huh7 cells served as a positive control.

Supplementary Figure 3. Global summary of detected features on mRNA and miRNA microarrays.

Supplementary Table 2: (A) Enrichment analysis. Tissue-specific miRNAs (Figure 1C, Venn diagram) were submitted to the MiEAA tool [55]. Expressed miRNAs were chosen as a reference set. Cell type-specific miRNAs were detected for 2 tissues: epithelial cells for colon cell lines (FDR=2.5e-3) and hepatocytes for liver cell lines (FDR=2.0e-2). **(B) CoExpress analysis.** Inverse correlation with a high coexpression score (CE) of genes and miRNAs indicates potential functional interactions. The very low TargetScan scores for such pairs are also listed, not predicting interactions.

Supplementary Figure 4. ICA analysis. Members of RIC1 and MIC1 are shown. RIC1 is activated in healthy cells, shows lower weights in cancer cell lines and is linked to immune response (also see Figure 3). MIC1 shows opposite profiles with higher weights in cancer.

Supplementary Figure 5. Gene expression in TCGA data sets. Comparison of TCGA data of log2 (normalized counts) expression levels of commonly differentially expressed mRNAs in matched normal (N) and tumor (T) tissues from bladder (N = 19), breast (N = 75), colon (N = 26), colorectal (N = 30), esophageal (N = 11), head and neck (N = 43), liver (N = 50), lung (N = 109), prostate (N = 52) and stomach (N = 32) cancer TCGA data. Error bars represent standard deviations. Stars show statistical significance of Wilcoxon matched-pairs signed rank test: * p-value < 0.05, ** p-value < 0.01, *** p-value < 0.001, **** p-value < 0.0001. Red outlines indicate higher expression in cancer compared to normal tissue and blue outlines show lower expression in tumors compared to normal tissue in unstimulated cells (if p-values < 0.001).

Supplementary Figure 6. GSEA. Gene set enrichment analysis was performed using the t values of differential gene expression for HIL6 and IFNγ in one cell line of each tissue (A375, HCT116 and Huh7) with ClusterProfiler [56].

Supplementary Figure 7. PCA analysis of cytokine-specific genes. Identification of transcripts that are affected by IL6-type or IFN-γ-type cytokines only or that are counter-regulated are boxed to highlight the different groups of genes.

Supplementary Table 3. List of cytokine-specific genes. List of transcripts of liver cells that are affected by IL6-type or IFN-γ-type cytokines only or that are counter-regulated by these treatments. The genes marked in blue or red were present in the lists of validated IFNγ- or IL6-type-cytokine-regulated genes, respectively [38].

References

1. P. Carninci, T. Kasukawa, S. Katayama, J. Gough, M. C. Frith, N. Maeda, R. Oyama, T. Ravasi, B. Lenhard, C. Wells, et al. (2005). The transcriptional landscape of the mammalian genome. *Science*; 309:1559-1563.
2. M. Cieslik and A. M. Chinnaiyan. (2018). Cancer transcriptome profiling at the juncture of clinical translation. *Nat Rev Genet*; 19:93-109.

3. N. Ludwig, P. Leidinger, K. Becker, C. Backes, T. Fehlmann, C. Pallasch, S. Rheinheimer, B. Meder, C. Stahler, E. Meese, et al. (2016). Distribution of miRNA expression across human tissues. *Nucleic Acids Res*; 44:3865-3877.
4. J. N. Weinstein and Y. Pommier. (2003). Transcriptomic analysis of the NCI-60 cancer cell lines. *C R Biol*; 326:909-920.
5. D. R. Robinson, Y. M. Wu, R. J. Lonigro, P. Vats, E. Cobain, J. Everett, X. Cao, E. Rabban, C. Kumar-Sinha, V. Raymond, et al. (2017). Integrative clinical genomics of metastatic cancer. *Nature*; 548:297-303.
6. J. E. Staunton, D. K. Slonim, H. A. Coller, P. Tamayo, M. J. Angelo, J. Park, U. Scherf, J. K. Lee, W. O. Reinhold, J. N. Weinstein, et al. (2001). Chemosensitivity prediction by transcriptional profiling. *Proc Natl Acad Sci U S A*; 98:10787-10792.
7. D. V. Kalvakolanu. (2019). The "Yin-Yang" of cytokines in cancer. *Cytokine*; 118:1-2.
8. S. Kany, J. T. Vollrath and B. Relja. (2019). Cytokines in Inflammatory Disease. *Int J Mol Sci*; 20.
9. C. Haan, S. Kreis, C. Margue and I. Behrmann. (2006). Jaks and cytokine receptors--an intimate relationship. *Biochem Pharmacol*; 72:1538-1546.
10. J. E. Darnell. (2005). Validating Stat3 in cancer therapy. *Nat Med*; 11:595-596.
11. L. Avalle, S. Pensa, G. Regis, F. Novelli and V. Poli. (2012). STAT1 and STAT3 in tumorigenesis: A matter of balance. *JAKSTAT*; 1:65-72.
12. G. P. Dunn, C. M. Koebel and R. D. Schreiber. (2006). Interferons, immunity and cancer immunoediting. *Nat Rev Immunol*; 6:836-848.
13. J. Hayes, P. P. Peruzzi and S. Lawler. (2014). MicroRNAs in cancer: biomarkers, functions and therapy. *Trends Mol Med*; 20:460-469.
14. P. Paul, A. Chakraborty, D. Sarkar, M. Langthasa, M. Rahman, M. Bari, R. S. Singha, A. K. Malakar and S. Chakraborty. (2018). Interplay between miRNAs and human diseases. *J Cell Physiol*; 233:2007-2018.
15. M. Kirchmeyer, F. A. Servais, M. Hamdorf, P. V. Nazarov, A. Ginolhac, R. Halder, L. Vallar, M. Glanemann, C. Rubie, F. Lammert, et al. (2018). Cytokine-mediated modulation of the hepatic miRNome: miR-146b-5p is an IL-6-inducible miRNA with multiple targets. *J Leukoc Biol*; 104:987-1002.
16. I. Kozar, G. Cesi, C. Margue, D. Philippidou and S. Kreis. (2017). Impact of BRAF kinase inhibitors on the miRNomes and transcriptomes of melanoma cells. *Biochim Biophys Acta Gen Subj*; 1861:2980-2992.
17. S. Reinsbach, P. V. Nazarov, D. Philippidou, M. Schmitt, A. Wienecke-Baldacchino, A. Muller, L. Vallar, I. Behrmann and S. Kreis. (2012). Dynamic regulation of microRNA expression following interferon-gamma-induced gene transcription. *RNA Biol*; 9:978-989.
18. M. J. Schmitt, D. Philippidou, S. E. Reinsbach, C. Margue, A. Wienecke-Baldacchino, D. Nashan, I. Behrmann and S. Kreis. (2012). Interferon-gamma-induced activation of Signal Transducer and Activator of Transcription 1 (STAT1) up-regulates the tumor suppressing microRNA-29 family in melanoma cells. *Cell Commun Signal*; 10:41.
19. F. A. Servais, M. Kirchmeyer, M. Hamdorf, N. W. E. Minoungou, S. Rose-John, S. Kreis, C. Haan and I. Behrmann. (2019). Modulation of the IL-6-Signaling Pathway in Liver Cells by miRNAs Targeting gp130, JAK1, and/or STAT3. *Mol Ther Nucleic Acids*; 16:419-433.
20. W. Si, J. Shen, H. Zheng and W. Fan. (2019). The role and mechanisms of action of microRNAs in cancer drug resistance. *Clin Epigenetics*; 11:25.
21. D. Loffler, K. Brocke-Heidrich, G. Pfeifer, C. Stocsits, J. Hackermuller, A. K. Kretzschmar, R. Burger, M. Gramatzki, C. Blumert, K. Bauer, et al. (2007). Interleukin-6 dependent survival of multiple myeloma cells involves the Stat3-mediated induction of microRNA-21 through a highly conserved enhancer. *Blood*; 110:1330-1333.
22. C. H. Yang, J. Yue, M. Fan and L. M. Pfeffer. (2010). IFN induces miR-21 through a signal transducer and activator of transcription 3-dependent pathway as a suppressive negative feedback on IFN-induced apoptosis. *Cancer Res*; 70:8108-8116.
23. C. H. Yang, J. Yue, S. R. Pfeffer, C. R. Handorf and L. M. Pfeffer. (2011). MicroRNA miR-21 regulates the metastatic behavior of B16 melanoma cells. *J Biol Chem*; 286:39172-39178.
24. D. Iliopoulos, S. A. Jaeger, H. A. Hirsch, M. L. Bulyk and K. Struhl. (2010). STAT3 activation of miR-21 and miR-181b-1 via PTEN and CYLD are part of the epigenetic switch linking inflammation to cancer. *Mol Cell*; 39:493-506.
25. D. P. Bartel. (2018). Metazoan MicroRNAs. *Cell*; 173:20-51.
26. Y. Peng and C. M. Croce. (2016). The role of MicroRNAs in human cancer. *Signal Transduct Target Ther*; 1:15004.
27. C. Haan and I. Behrmann. (2007). A cost effective non-commercial ECL-solution for Western blot detections yielding strong signals and low background. *Journal of immunological methods*; 318:11-19.
28. S. J. Le, J.; Husson, F. . (2008). FactoMineR: An R package for multivariate analysis. *Journal of statistical software*; 25:1-18.

29. A. M. Kassambara, M. . (2017). factoextra: Extract and Visualize the Results of Multivariate Data Analyses. R package version 1.0.4. .
30. H. Wickham. (2009). ggplot2: Elegant Graphics for Data Analysis, Springer-Verlag, New York.

31. H. Wickham. (2017). tidyverse: Easily Install and Load 'Tidyverse' Packages. R package version 1.0.0. .
32. P. V. Nazarov, A. K. Wienecke-Baldacchino, A. Zinovyev, U. Czerwinska, A. Muller, D. Nashan, G. Dittmar, F. Azuaje and S. Kreis. (2019). Deconvolution of transcriptomes and miRNomes by independent component analysis provides insights into biological processes and clinical outcomes of melanoma patients. *BMC Med Genomics*; 12:132.
33. P. V. Nazarov, S. E. Reinsbach, A. Muller, N. Nicot, D. Philippidou, L. Vallar and S. Kreis. (2013). Interplay of microRNAs, transcription factors and target genes: linking dynamic expression changes to function. *Nucleic Acids Res*; 41:2817-2831.
34. A. Biton, I. Bernard-Pierrot, Y. Lou, C. Krucker, E. Chapeaublanc, C. Rubio-Perez, N. Lopez-Bigas, A. Kamoun, Y. Neuzillet, P. Gestraud, et al. (2014). Independent component analysis uncovers the landscape of the bladder tumor transcriptome and reveals insights into luminal and basal subtypes. *Cell Rep*; 9:1235-1245.
35. S. I. Lee and S. Batzoglou. (2003). Application of independent component analysis to microarrays. *Genome Biol*; 4:R76.
36. M. Kurowska-Stolarska, S. Alivernini, E. G. Melchor, A. Elmesmari, B. Tolusso, C. Tange, L. Petricca, D. S. Gilchrist, G. Di Sante, C. Keijzer, et al. (2017). MicroRNA-34a dependent regulation of AXL controls the activation of dendritic cells in inflammatory arthritis. *Nat Commun*; 8:15877.
37. G. Mudduluru, P. Ceppi, R. Kumarswamy, G. V. Scagliotti, M. Papotti and H. Allgayer. (2011). Regulation of Axl receptor tyrosine kinase expression by miR-34a and miR-199a/* in solid cancer. *Oncogene*; 30:2888-2899.
38. C. Rolvering, A. D. Zimmer, A. Ginolhac, C. Margue, M. Kirchmeyer, F. Servais, H. M. Hermanns, S. Hergovits, P. V. Nazarov, N. Nicot, et al. (2018). The PD-L1- and IL6-mediated dampening of the IL27/STAT1 anticancer responses are prevented by alpha-PD-L1 or alpha-IL6 antibodies. *J Leukoc Biol*; 104:969-985.
39. D. E. Levy and C. K. Lee. (2002). What does Stat3 do? *J Clin Invest*; 109:1143-1148.
40. C. G. Son, S. Bilke, S. Davis, B. T. Greer, J. S. Wei, C. J. Whiteford, Q. R. Chen, N. Cenacchi and J. Khan. (2005). Database of mRNA gene expression profiles of multiple human organs. *Genome research*; 15:443-450.
41. T. Yoshimura, S. Toyoda, S. Kuramochi-Miyagawa, T. Miyazaki, S. Miyazaki, F. Tashiro, E. Yamato, T. Nakano and J. Miyazaki. (2009). Gtsf1/Cue110, a gene encoding a protein with two copies of a CHHC Zn-finger motif, is involved in spermatogenesis and retrotransposon suppression in murine testes. *Developmental biology*; 335:216-227.
42. I. V. Litvinov, B. Cordeiro, Y. Huang, H. Zargham, K. Pehr, M. A. Dore, M. Gilbert, Y. Zhou, T. S. Kupper and D. Sasseville. (2014). Ectopic expression of cancer-testis antigens in cutaneous T-cell lymphoma patients. *Clinical cancer research : an official journal of the American Association for Cancer Research*; 20:3799-3808.
43. K. M. Hatle, P. Gummadidala, N. Navarsa, E. Bernardo, J. Dodge, B. Silverstrim, K. Fortner, E. Burg, B. T. Suratt, J. Hammer, et al. (2013). MCJ/DnaJC15, an endogenous mitochondrial repressor of the respiratory chain that controls metabolic alterations. *Molecular and cellular biology*; 33:2302-2314.
44. D. Sinha and P. D'Silva. (2014). Chaperoning mitochondrial permeability transition: regulation of transition pore complex by a J-protein, DnaJC15. *Cell death & disease*; 5:e1101.
45. V. Shridhar, K. C. Bible, J. Staub, R. Avula, Y. K. Lee, K. Kalli, H. Huang, L. C. Hartmann, S. H. Kaufmann and D. I. Smith. (2001). Loss of expression of a new member of the DNAJ protein family confers resistance to chemotherapeutic agents used in the treatment of ovarian cancer. *Cancer Res*; 61:4258-4265.
46. K. M. Hatle, W. Neveu, O. Dienz, S. Rymarchyk, R. Barrantes, S. Hale, N. Farley, K. M. Lounsbury, J. P. Bond, D. Taatjes, et al. (2007). Methylation-controlled J protein promotes c-Jun degradation to prevent ABCB1 transporter expression. *Molecular and cellular biology*; 27:2952-2966.
47. J. Bromberg. (2002). Stat proteins and oncogenesis. *J Clin Invest*; 109:1139-1142.
48. K. Friedrich, H. Dolznig, X. Han and R. Moriggl. (2017). Steering of carcinoma progression by the YIN/YANG interaction of STAT1/STAT3. *Biosci Trends*; 11:1-8.
49. U. Boehm, T. Klamp, M. Groot and J. C. Howard. (1997). Cellular responses to interferon-gamma. *Annu Rev Immunol*; 15:749-795.
50. B. Burkholder, R. Y. Huang, R. Burgess, S. Luo, V. S. Jones, W. Zhang, Z. Q. Lv, C. Y. Gao, B. L. Wang, Y. M. Zhang, et al. (2014). Tumor-induced perturbations of cytokines and immune cell networks. *Biochim Biophys Acta*; 1845:182-201.
51. L. Yan, F. Xu and C. L. Dai. (2018). Relationship between epithelial-to-mesenchymal transition and the inflammatory microenvironment of hepatocellular carcinoma. *J Exp Clin Cancer Res*; 37:203.
52. X. Wang, S. Abraham, J. A. G. McKenzie, N. Jeffs, M. Swire, V. B. Tripathi, U. F. O. Luhmann, C. A. K. Lange, Z. Zhai, H. M. Arthur, et al. (2013). LRG1 promotes angiogenesis by modulating endothelial TGF-beta signalling. *Nature*; 499:306-311.

53. Z. Kiss, M. M. and M. P. Ghosh. (2020). Non-circadian aspects of BHLHE40 cellular function in cancer. *Genes & Cancer*.
54. H. Liu, N. Wu, Z. Zhang, X. Zhong, H. Zhang, H. Guo, Y. Nie and Y. Liu. (2019). Long Non-coding RNA LINC00941 as a Potential Biomarker Promotes the Proliferation and Metastasis of Gastric Cancer. *Front Genet*; 10:5.
55. F. Kern, T. Fehlmann, J. Solomon, L. Schwed, N. Grammes, C. Backes, K. Van Keuren-Jensen, D. W. Craig, E. Meese and A. Keller. (2020). miEAA 2.0: integrating multi-species microRNA enrichment analysis and workflow management systems. *Nucleic Acids Res*; 48:W521-W528.
56. G. Yu, L. G. Wang, Y. Han and Q. Y. He. (2012). clusterProfiler: an R package for comparing biological themes among gene clusters. *OMICS*; 16:284-287.

Credit Author statement
MK, FS: investigation, validation, formal analysis, visualization; AG, PN: data curation, visualization, formal analysis; CM, DP, NN: investigation, validation; IB: Conceptualization, funding acquisition, supervision; CH: writing of original draft, Conceptualization, formal analysis, methodology; SK: Conceptualization, funding acquisition, supervision, writing of original draft, project administration.

Declaration of interests

☒ The authors declare that they have no known competing financial interests or personal relationships that could have appeared to influence the work reported in this paper.

☐The authors declare the following financial interests/personal relationships which may be considered as potential competing interests:

Research highlights:

- Characterization of transcriptomic changes in cancer cells of 3 different tissues and following exposure to 4 distinct cytokines.
- IFNγ-type/STAT1 responses mostly involved in anti-cancer signalling networks.
- IL6-type/STAT3-activated gene profiles predominantly found in oncogenic signalling.
- Liver cells had stronger responses to cytokines than skin and colon cells.
- Detailed investigation of gene regulation responses following cytokine-triggered activation of either STAT1 or STAT3 transcription factors.

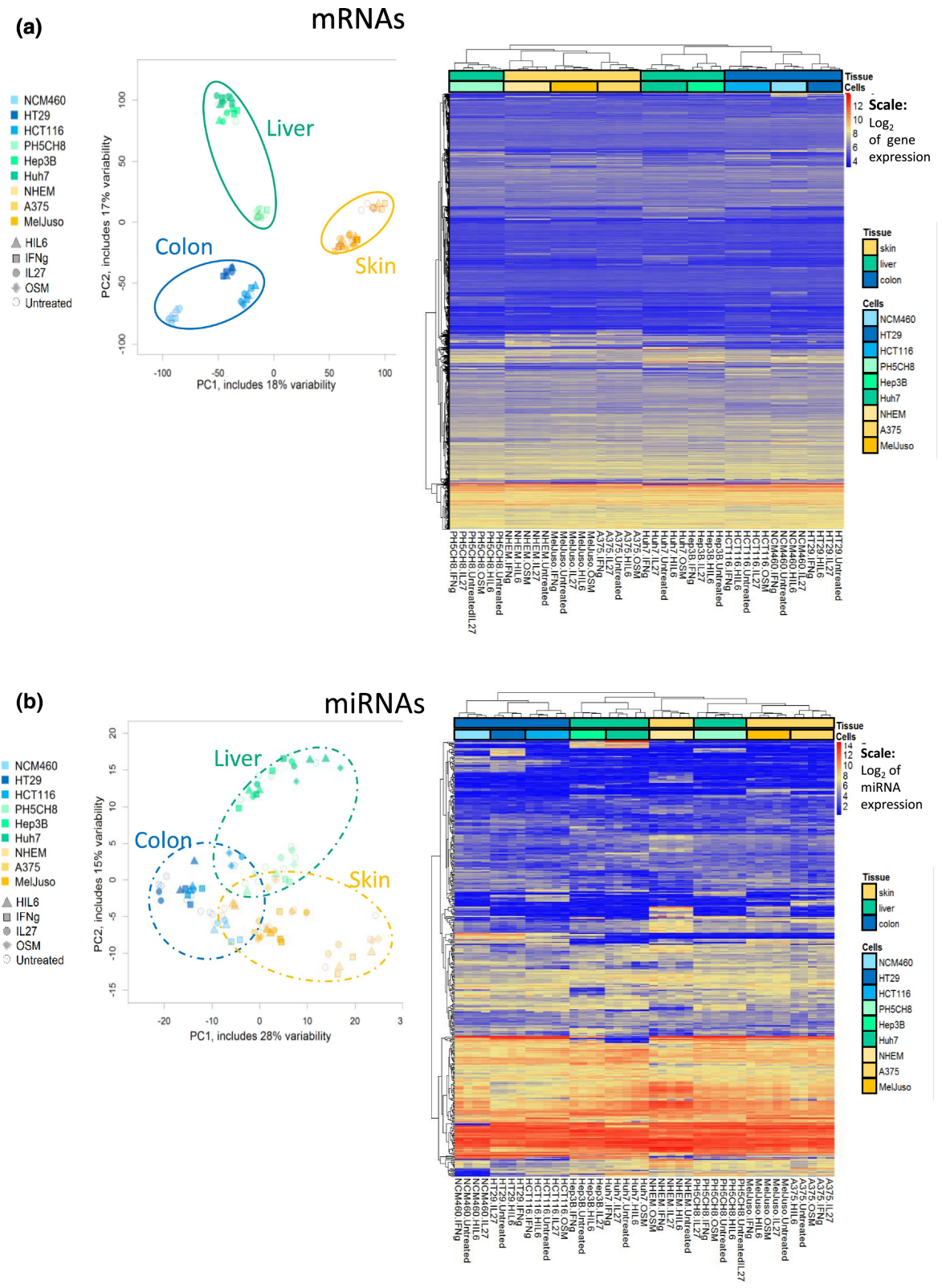
(a)
mRNAs
NCM460
HT29
HCT116
PH5CH8
Hep3B
Huh7
NHEM
A375
MelJuso
HIL6
IFNg
IL27
OSM
Untreated
Liver
Colon
Skin
PC2, includes 17% variability
PC1, includes 18% variability
Tissue
Cells
Scale:
Log2 of gene expression
skin
liver
colon
(b)
miRNAs
PC2, includes 15% variability
PC1, includes 28% variability
Scale:
Log2 of miRNA expression

Figure 1ab

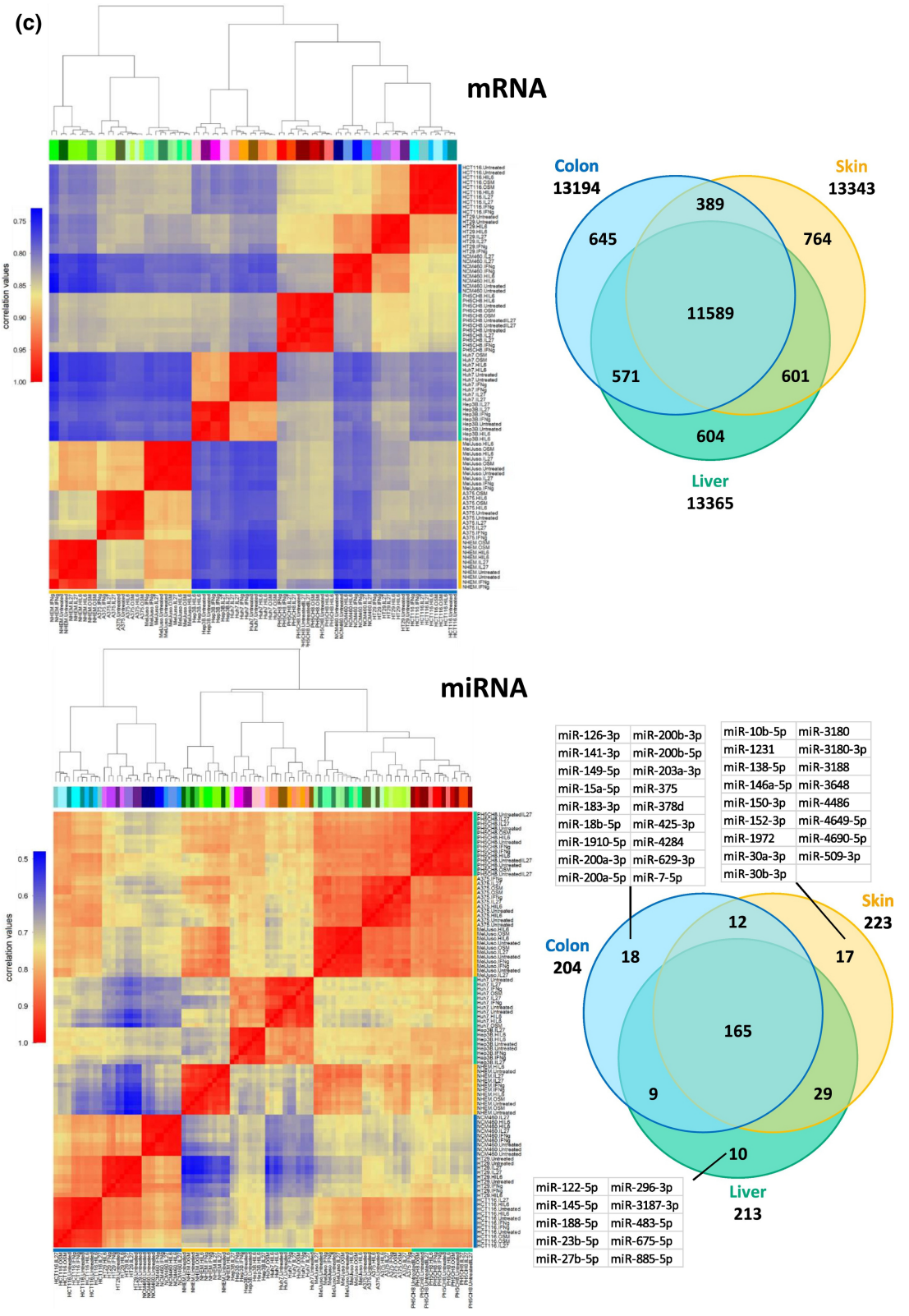
(c)
mRNA
correlation values
0.75
0.80
0.85
0.90
0.95
1.00
Colon
13194
Skin
13343
Liver
13365
645
389
764
11589
571
601
604
miRNA
correlation values
0.5
0.6
0.7
0.8
0.9
1.0
miR-126-3p
miR-141-3p
miR-149-5p
miR-15a-5p
miR-183-3p
miR-18b-5p
miR-1910-5p
miR-200a-3p
miR-200a-5p
miR-200b-3p
miR-200b-5p
miR-203a-3p
miR-375
miR-378d
miR-425-3p
miR-4284
miR-629-3p
miR-7-5p
miR-10b-5p
miR-1231
miR-138-5p
miR-146a-5p
miR-150-3p
miR-152-3p
miR-1972
miR-30a-3p
miR-30b-3p
miR-3180
miR-3180-3p
miR-3188
miR-3648
miR-4486
miR-4649-5p
miR-4690-5p
miR-509-3p
Colon
204
Skin
223
Liver
213
18
12
17
165
9
29
10
miR-122-5p
miR-145-5p
miR-188-5p
miR-23b-5p
miR-27b-5p
miR-296-3p
miR-3187-3p
miR-483-5p
miR-675-5p
miR-885-5p

Figure 1c

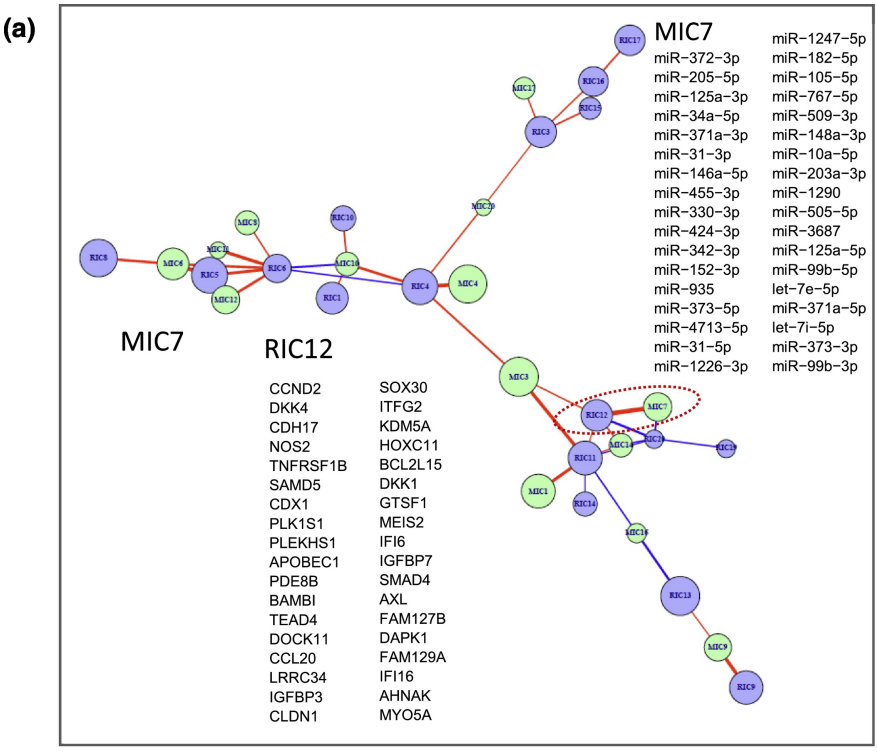
(a)
MIC7
miR−372−3p
miR−205−5p
miR−125a−3p
miR−34a−5p
miR−371a−3p
miR−31−3p
miR−146a−5p
miR−455−3p
miR−330−3p
miR−424−3p
miR−342−3p
miR−152−3p
miR−935
miR−373−5p
miR−4713−5p
miR−31−5p
miR−1226−3p
miR−1247−5p
miR−182−5p
miR−105−5p
miR−767−5p
miR−509−3p
miR−148a−3p
miR−10a−5p
miR−203a−3p
miR−1290
miR−505−5p
miR−3687
miR−125a−5p
miR−99b−5p
let−7e−5p
miR−371a−5p
let−7i−5p
miR−373−3p
miR−99b−3p
MIC7
RIC12
CCND2
DKK4
CDH17
NOS2
TNFRSF1B
SAMD5
CDX1
PLK1S1
PLEKHS1
APOBEC1
PDE8B
BAMBI
TEAD4
DOCK11
CCL20
LRRC34
IGFBP3
CLDN1
SOX30
ITFG2
KDM5A
HOXC11
BCL2L15
DKK1
GTSF1
MEIS2
IFI6
IGFBP7
SMAD4
AXL
FAM127B
DAPK1
FAM129A
IFI16
AHNAK
MYO5A

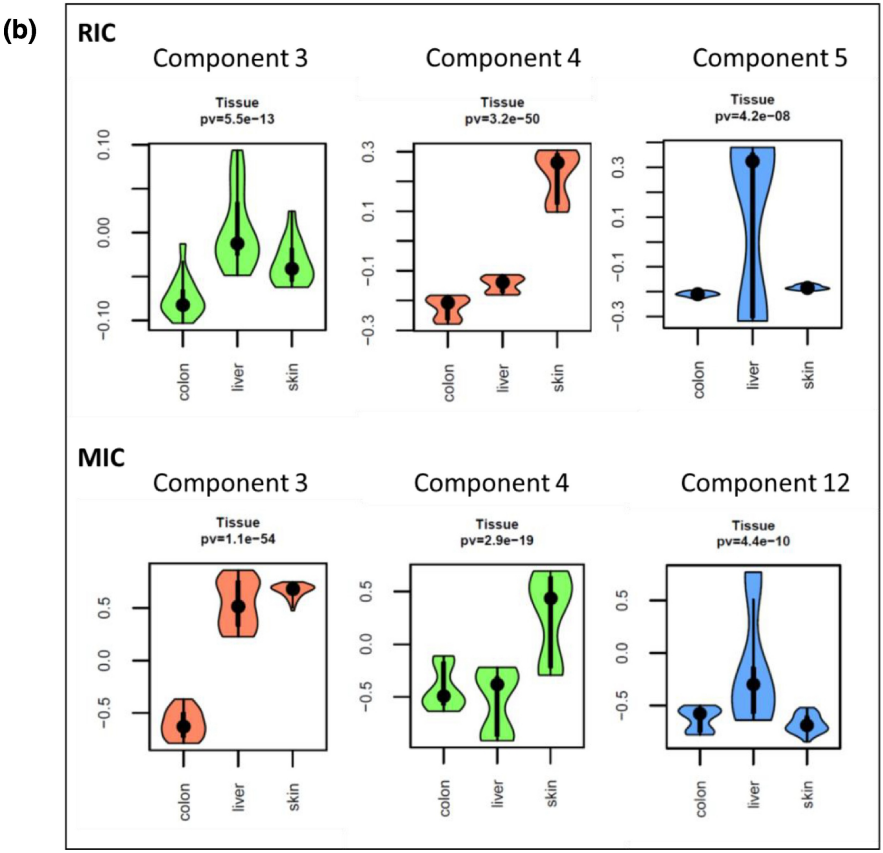
(b)
RIC
Component 3
Component 4
Component 5
Tissue
pv=5.5e−13
pv=3.2e−50
pv=4.2e−08
colon
liver
skin
MIC
Component 3
Component 4
Component 12
Tissue
pv=1.1e−54
pv=2.9e−19
pv=4.4e−10
colon
liver
skin

Figure 2

(a)

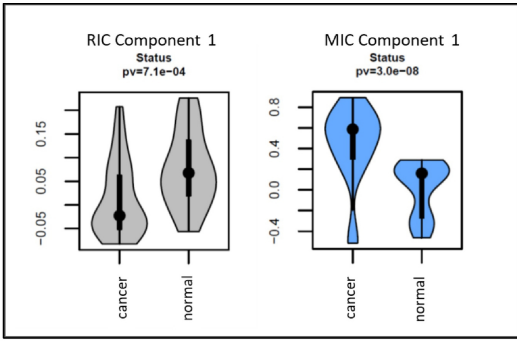

(b)

mRNA		Signif	Up	Down
Colon	HT29	1510	744	766
	HCT116	2331	979	1352
	Common	821	271	527
Liver	Hep3B	2442	1097	1345
	Huh-7	2758	1346	1414
	Common	1580	657	872
Skin	MelJuso	1592	691	901
	A375	2178	1062	1116
	Common	866	278	554
Cancer vs Healthy		28	1	4

(c)

Genes	Colon		Liver		Skin		Function
	HCT116	HT29	Hep3B	Huh-7	A375	MelJuso	
FAM171B	1.59	1.99	1.95	1.09	1.17	1.35	Transmembrane protein
FAM21B	-1.33	-1.1	-1.06	-1.26	-1.44	-1.04	Involved in endocytosis
FAM43A	-1.11	-1.6	-1.03	-1.29	-1.45	-1.7	Function unknown
OAS1	-2.84	-1.1	-1.83	-1.77	-2.57	-2.71	IFN-regulated proapoptotic gene involved in antiviral response, associated with many diseases
REPS2	-1.58	-1.04	-1.48	-1.54	-1.67	-1.54	Involved in endocytosis of growth factor receptors
GTSF1	6.52	4.09	2.26	5.78	6.46	0.67	Involved in suppression of retrotransposon transcription in male germ cells
DNAJC15	-1.43	-1.9	-4.54	-0.96	-1.85	-1.71	Negative regulator of mitochondrial respiratory chain, linked to apoptosis and enhanced drug sensitivity

Figure 3

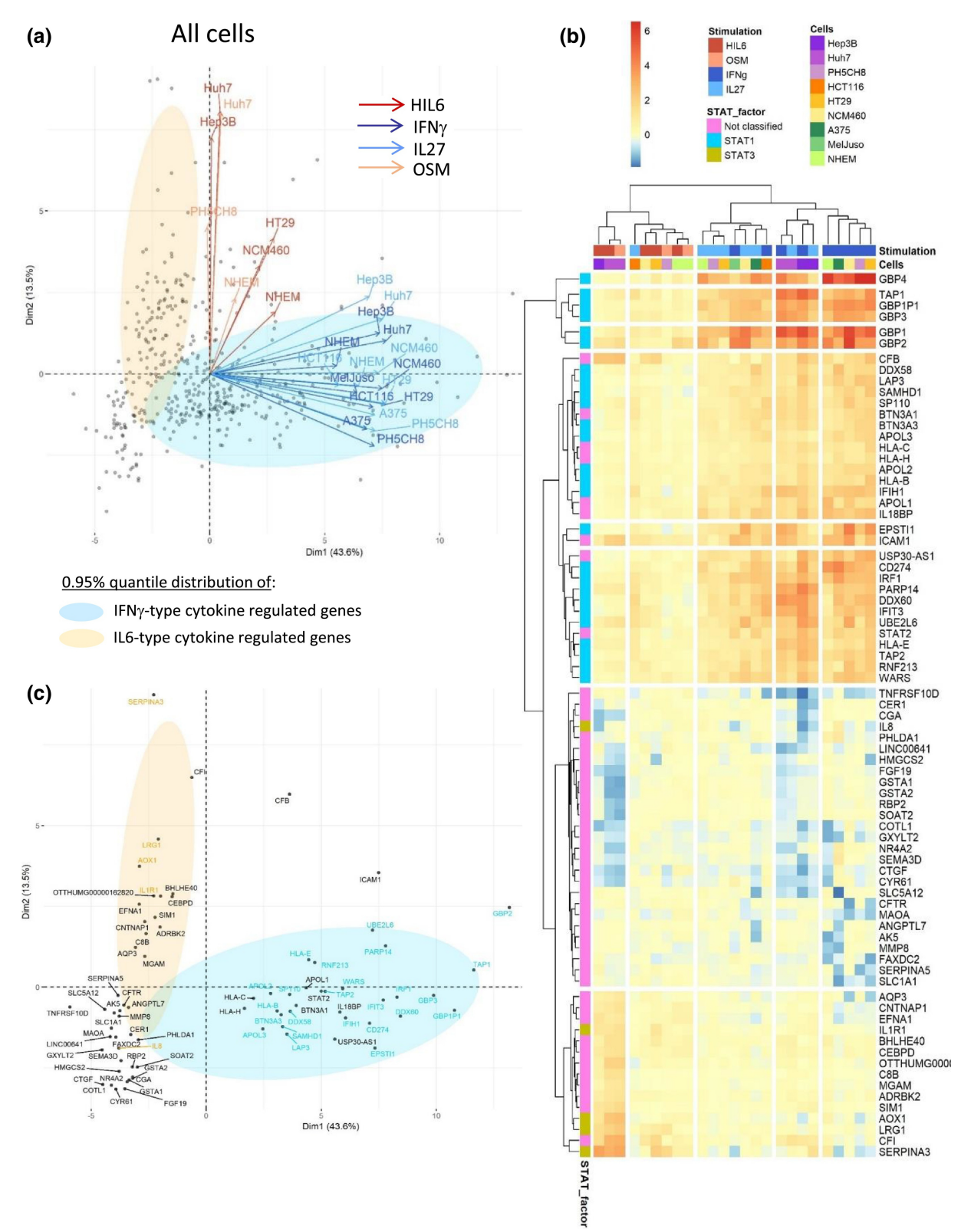
(a)
All cells
HIL6
IFNγ
IL27
OSM
Huh7
Huh7
Hep3B
PH5CH8
HT29
NCM460
NHEM
NHEM
Hep3B
Huh7
Hep3B
Huh7
NHEM
NCM460
HCT116
NHEM
NCM460
MelJuso
HT29
HCT116
HT29
A375
A375
PH5CH8
PH5CH8
Dim2 (13.5%)
Dim1 (43.6%)
0.95% quantile distribution of:
IFNγ-type cytokine regulated genes
IL6-type cytokine regulated genes
(b)
Stimulation
HIL6
OSM
IFNg
IL27
STAT_factor
Not classified
STAT1
STAT3
Cells
Hep3B
Huh7
PH5CH8
HCT116
HT29
NCM460
A375
MelJuso
NHEM
Stimulation
Cells
GBP4
TAP1
GBP1P1
GBP3
GBP1
GBP2
CFB
DDX58
LAP3
SAMHD1
SP110
BTN3A1
BTN3A3
APOL3
HLA-C
HLA-H
APOL2
HLA-B
IFIH1
APOL1
IL18BP
EPSTI1
ICAM1
USP30-AS1
CD274
IRF1
PARP14
DDX60
IFIT3
UBE2L6
STAT2
HLA-E
TAP2
RNF213
WARS
TNFRSF10D
CER1
CGA
IL8
PHLDA1
LINC00641
HMGCS2
FGF19
GSTA1
GSTA2
RBP2
SOAT2
COTL1
GXYLT2
NR4A2
SEMA3D
CTGF
CYR61
SLC5A12
CFTR
MAOA
ANGPTL7
AK5
MMP8
FAXDC2
SERPINA5
SLC1A1
AQP3
CNTNAP1
EFNA1
IL1R1
BHLHE40
CEBPD
OTTHUMG000
C8B
MGAM
ADRBK2
SIM1
AOX1
LRG1
CFI
SERPINA3
STAT_factor
(c)
SERPINA3
CFI
CFB
LRG1
AOX1
ICAM1
OTTHUMG00000162820
IL1R1
BHLHE40
CEBPD
EFNA1
SIM1
GBP2
CNTNAP1
ADRBK2
UBE2L6
C8B
AQP3
MGAM
HLA-E
PARP14
TAP1
RNF213
SERPINA5
APOL1
WARS
SLC5A12
CFTR
APOL2
IRF1
HLA-C
TAP2
AK5
ANGPTL7
STAT2
GBP3
TNFRSF10D
HLA-B
IL18BP
IFIT3
HLA-H
BTN3A1
DDX60
MMP8
GBP1P1
SLC1A1
BTN3A3
DDX58
CER1
IFIH1
MAOA
APOL3
CD274
PHLDA1
SAMHD1
USP30-AS1
LINC00641
FAXDC2
IL8
LAP3
EPSTI1
GXYLT2
SEMA3D
RBP2
SOAT2
HMGCS2
GSTA2
CTGF
NR4A2
CGA
COTL1
GSTA1
CYR61
FGF19
Dim2 (13.5%)
Dim1 (43.6%)

Figure 4

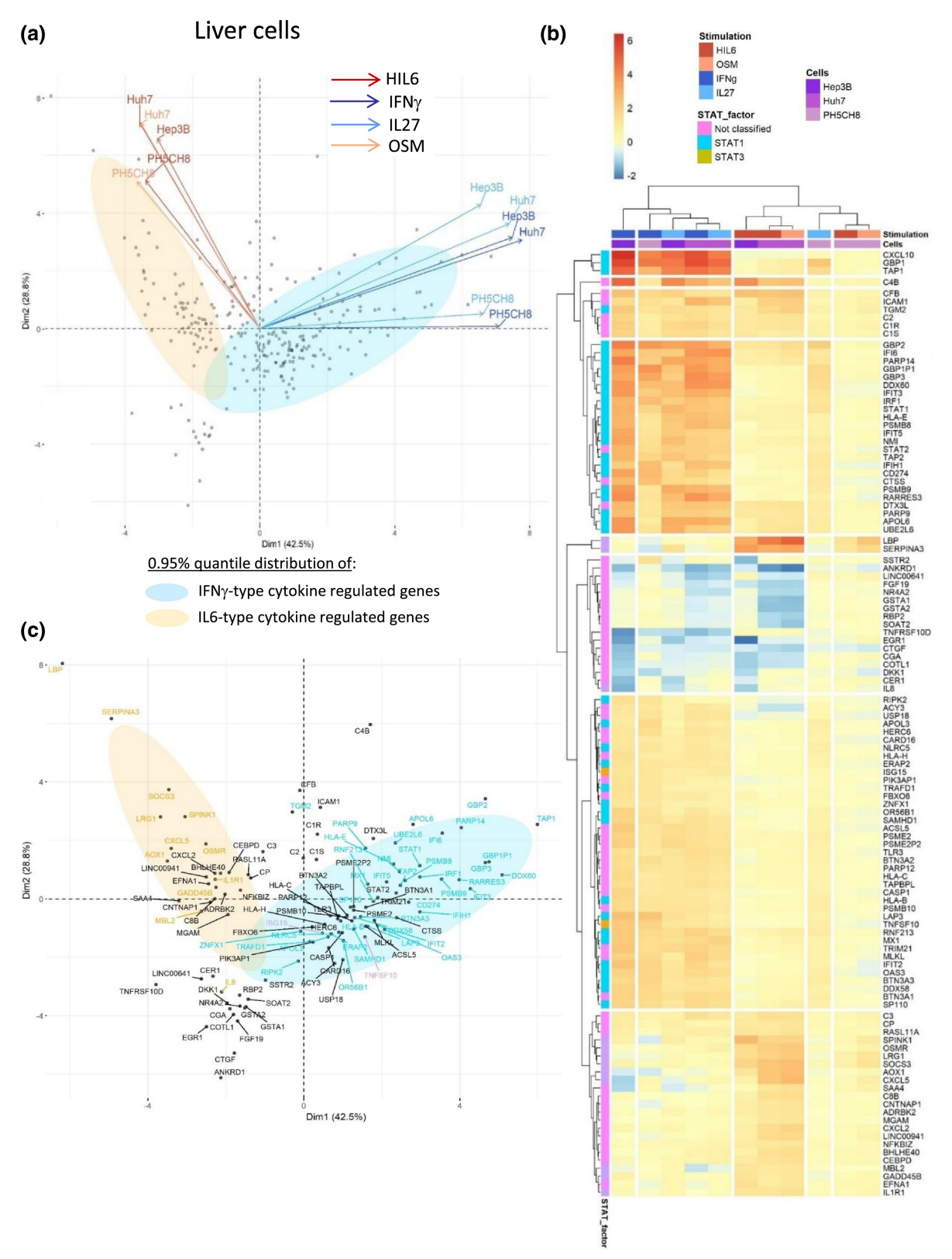
(a)
Liver cells
HIL6
IFNγ
IL27
OSM
Huh7
Hep3B
PH5CH8
Dim1 (42.5%)
Dim2 (28.8%)
0.95% quantile distribution of:
IFNγ-type cytokine regulated genes
IL6-type cytokine regulated genes
(b)
Stimulation
HIL6
OSM
IFNg
IL27
Cells
Hep3B
Huh7
PH5CH8
STAT_factor
Not classified
STAT1
STAT3
(c)
Dim1 (42.5%)
Dim2 (28.8%)

Figure 5

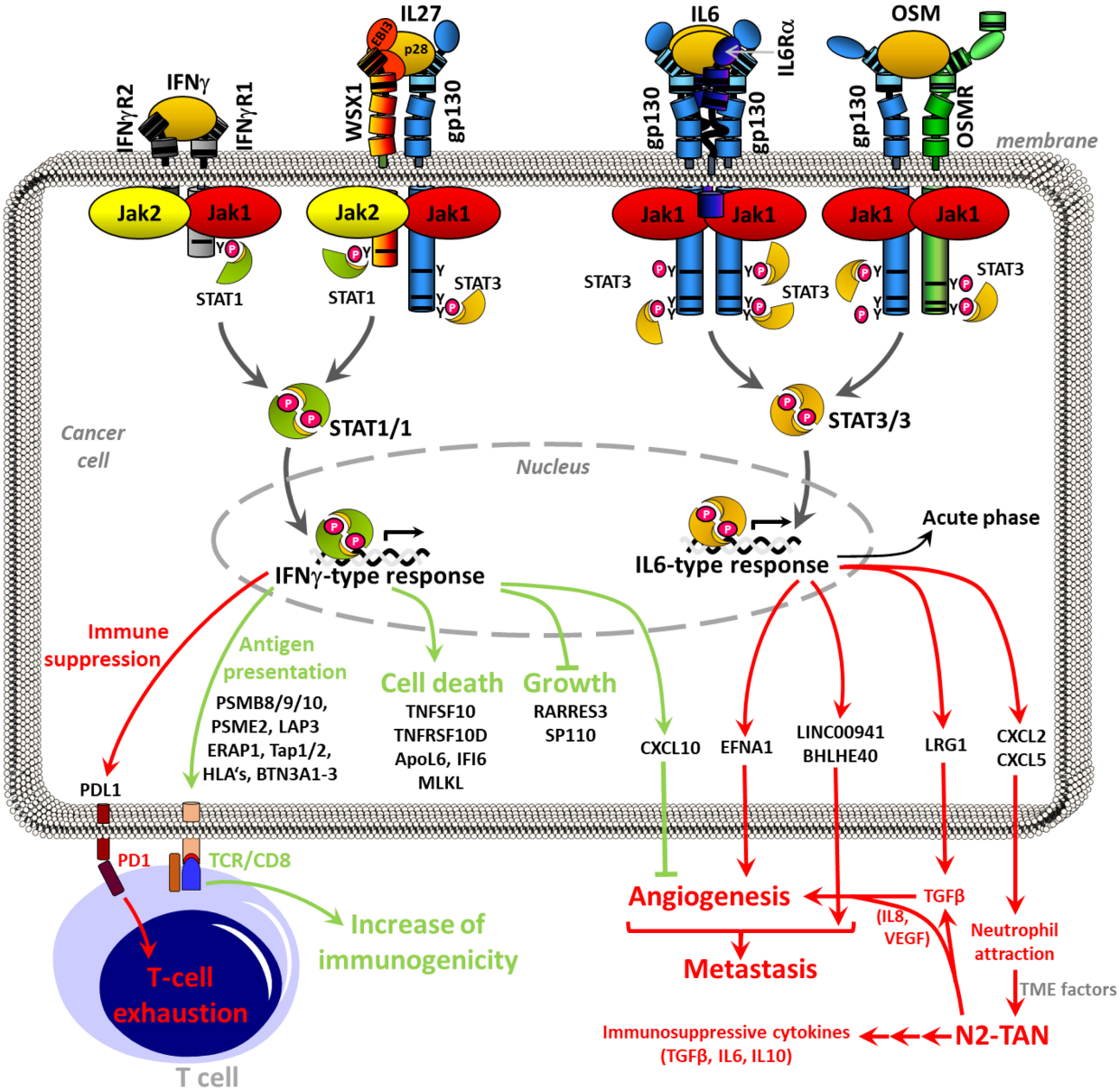
IL27
EBI3
p28
IFNγ
IFNγR2
IFNγR1
WSX1
gp130
IL6
IL6Rα
gp130
gp130
OSM
OSMR
membrane
Jak2
Jak1
Jak2
Jak1
Jak1
Jak1
Jak1
Jak1
STAT1
STAT1
STAT3
STAT3
STAT3
STAT3
STAT1/1
STAT3/3
Cancer cell
Nucleus
IFNγ-type response
IL6-type response
Acute phase
Immune suppression
Antigen presentation
PSMB8/9/10, PSME2, LAP3 ERAP1, Tap1/2, HLA's, BTN3A1-3
Cell death
TNFSF10 TNFRSF10D ApoL6, IFI6 MLKL
Growth
RARRES3 SP110
CXCL10
EFNA1
LINC00941 BHLHE40
LRG1
CXCL2 CXCL5
PDL1
PD1
TCR/CD8
T-cell exhaustion
T cell
Increase of immunogenicity
Angiogenesis
TGFβ
(IL8, VEGF)
Neutrophil attraction
Metastasis
TME factors
Immunosuppressive cytokines (TGFβ, IL6, IL10)
N2-TAN

Figure 6